Nanoscale

Accepted Manuscript

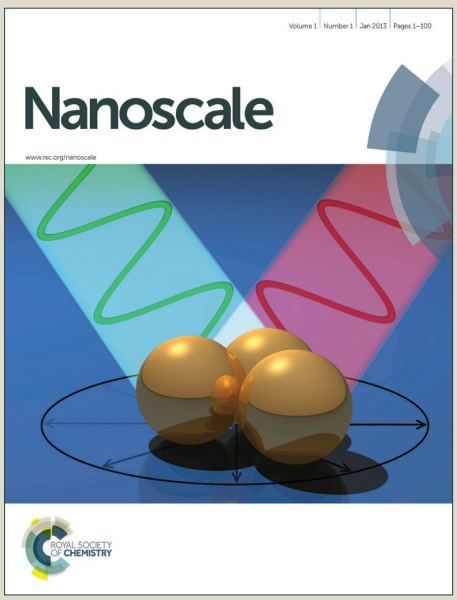

ROYAL SOCIETY OF CHEMISTRY

www.rsc.org/nanoscale

Photon Upconversion Sensitized Nanoprobes for Sensing and Imaging of pH

*Riikka Arppe, Tuomas Näreoja, Sami Nylund, Leena Mattsson, Sami Koho, Jessica M. Rosenholm, Tero Soukka, Michael Schäferling**

R. Arppe, S. Nylund, L. Mattsson, Prof. T. Soukka, Dr. M. Schäferling, Department of Biochemistry /Biotechnology, University of Turku, Tykistökatu 6A, FI-20520 Turku (Finland)
Email: Michael.schaeferling@utu.fi

T. Näreoja, S. Koho, Laboratory of Biophysics, Institute of Biomedicine and Medicity research laboratories, University of Turku, Tykistökatu 6A, 20520 Turku (Finland)

Dr. J.M. Rosenholm, Laboratory for Physical Chemistry, Åbo Akademi University, Porthansgatan 3, 20500 Turku (Finland)

KEYWORDS. pH, nanosensor, upconverting nanoparticle, upconversion photoluminescence resonance energy transfer

Table of Contents Entry

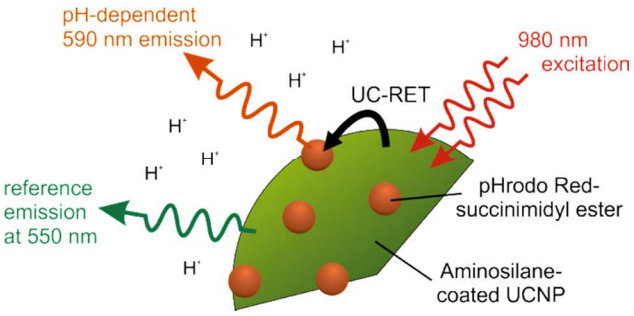

Ratiometric referenced luminescent pH nanosensors based on an upconversion resonance energy transfer (UC-RET) process enable imaging applications with NIR excitation.

Abstract

Acidic pH inside cells indicates cellular dysfunctions such as cancer. Therefore, the development of optical pH sensors for measuring and imaging intracellular pH is a demanding challenge. The available pH-sensitive probes are vulnerable to e.g. photobleaching or autofluorescence background in biological materials. Our approach circumvents these problems due to near infrared excitation and upconversion photoluminescence. We introduce a nanosensor based on upconversion resonance energy transfer (UC-RET) between an upconverting nanoparticle (UCNP) and a fluorogenic pH-dependent dye pHrodo™ Red that was covalently bound to the aminosilane surface of the nanoparticles. The sensitized fluorescence of the pHrodo™ Red dye increases strongly with decreasing pH. By referencing the pH-dependent emission of pHrodo™ Red with the pH-insensitive upconversion photoluminescence of the UCNP, we developed a pH-sensor which exhibits a dynamic range from pH 7.2 to 2.5. The applicability of the introduced pH nanosensor for pH imaging was demonstrated by imaging the two emission wavelengths of the nanoprobe in living HeLa cells with a confocal fluorescence microscope upon 980-nm

excitation. This demonstrates, that the presented pH-nanoprobe can be used as intracellular pH-sensor due to the unique features of UCNPs: excitation with deeply penetrating near-infrared light, high photostability, lack of autofluorescence and biocompatibility due to aminosilane coating.

1 Introduction

Luminescent methods for monitoring and imaging of intracellular pH play an important role in biomedical research. Abnormal acidic pH values are characteristic of cellular dysfunctions such as cancer, apoptosis and cell proliferation. Decreased pHs between 4 and 6 also occur in certain cellular compartments such as endosomes or lysosomes. A large variety of fluorescent indicators is available for measuring intracellular pH, particularly the manifold derivatives of fluorescein, benzoxanthene, cyanine, rhodamine, boron-dipyrromethene (BODIPY), or 8-hydroxypyrene-1,3,6-trisulfonic acid (HPTS).[1] Nevertheless, in the past years more and more attention was directed to the application of nanoparticles for pH sensing, for instance by attachment or incorporation of pH sensitive probes to polymer or silica beads. These nanoprobes have several advantages compared to pH indicators based on small organic molecules such as higher local brightness, higher photostability, shielding from interferences and the possibility to include reference dyes for ratiometric measurements.[2] Finally, the surface properties of nanoparticles can be modulated, so that they are cell permeable, e.g. by internalization via endocytosis[3] and can be targeted to cellular compartments or for in vivo imaging.[4-6]

The first polymer-based nanoparticles for intracellular pH measurement were developed by the group of Kopelman et al.[7] They consisted of fluorescein and a reference dye embedded in a polyacrylamide matrix. Other approaches followed to achieve internal referenced polymer

nanoprobes for pH.[8] Furthermore, polystyrene microspheres,[9] core/shell silica particles[2] or CdSe/ZnSe/ZnS quantum dots[10] have been applied to image pH inside living cells. Core/shell nanoparticles have been also utilized for the preparation of dual probes for pH and oxygen sensing.[11]

However, all these probes do not overcome one general problem of pH indicators in biological sample matrices: they have rather shortwave excitation and emission wavelengths, and the few available probes absorbing in the biological optical window in the far red or near-infrared (NIR) spectral range are prone to photobleaching. Therefore, we followed a different strategy for the design of luminescent nanoprobes for pH sensing that utilizes the advantages of upconversion photoluminescence, which is free of autofluorescence background and due to its NIR excitation particularly suited for measurements in complex biological samples such as whole blood,[12] and also for cellular or in vivo imaging.[13] Hexagonal nanocrystals of $NaYF_4$:Yb^{3+},Er^{3+} show high upconversion efficiency upon 980 nm excitation and two sharp luminescence emission bands in the green (~ 550 nm) and red (~ 660 nm) spectral range which are ideal for resonance energy transfer applications together with small-molecule organic dye acceptors such as Alexa Fluor 546[14], AF680[12,15], AF700[14], Rose Bengal[16], 4-((4-(2-aminoethylamino)naphthalen-1-yl)diazenyl) benzenesulfonic acid dihydrochloride[17], BOBO-3[18], Cy3[19], and Rhodamine B[20, 21]. Up to now only few examples are described in literature where photon upconversion materials are utilized in chemical sensors.[22] Upconverting nanoparticles (UCNPs) have been incorporated in polystyrene in combination with pH indicators to achieve optical sensors for ammonia[23] or carbon dioxide[24] that are based on a pH dependent inner filter effect on the UCNP emission. Though, this approach using planar sensor films is not applicable to intracellular or in vivo imaging purposes. Recently it was shown that UCNPs with a dendritic polyglutamic shell which

was functionalized with a meso-tetraphenylporphyrin derivative can act as a ratiometric probe for pH.[25] Thereby, protonation of the porphyrin leads to a shift of its absorption bands (Q-bands) and, therefore, to a change of their overlap with the two main UCNP emissions around 550 and 660 nm. This results in a ratiometric pH titration curve by measuring the intensities of both UCNP emissions. However, the energy transfer from the UCNP to the porphyrin occurs predominantly via an emission-reabsorption mechanism (inner filter effect of the porphyrin absorptions), as only minor change in the luminescence lifetimes of the UCNP emission could be observed.

Here we used a fluorogenic molecular pH probe which is covalently coupled to the surface of aminosilane coated UCNPs to achieve preferably a direct resonance energy transfer from the upconverter to the indicator. For that purpose, we selected pHrodo™ Red as indicator which absorption coincides with the green emission of the UCNP and its emission shows a strong increase in acidic pH, covering a broad dynamic range from pH 8 to pH 4 with a pKa around 6.5. Therefore, it is highly suitable for sensing and imaging of pH in acidic cellular compartments, e.g. for monitoring of endocytosis, phagocytosis or lysosomes. The functionalized UCNPs can be utilized as referenced probes by measuring the pH dependent fluorescence of the coupled indicator at 590 nm in relation to the insensitive luminescence emission of the UCNP around 550 nm. We also studied the influence of ionic strength on the pH response, the pH dependent aggregation behavior of the nanoparticles, their cellular uptake, and demonstrated their feasibility to fluorescence microscope imaging using a 980 nm laser as excitation source.

2 Results and Discussion

Preparation and characterization of UCNP-pHrodo™ Red-conjugate

Hexagonal $NaYF_4:Yb^{3+},Er^{3+}$ crystals with a diameter of 28 × 36 nm have been synthesized[26] (Figure 1) and coated with a thin aminosilane shell using a mixture of tetramethyl-orthosilicate and (N-(3-trimethoxysilyl)-propyl)ethylene diamine.[27] Then, the commercially available pH indicator pHrodo™ Red NHS ester was covalently coupled to the surface of the particles. It shows an absorption maximum at 555 nm and a pH dependent emission at 585 nm. The spectral properties and the chemical structure of the dye have been already revealed.[28] 67 nmol of dye per mg UCNP was used for the conjugation reaction and a 85 % yield was achieved which was estimated by comparison of direct fluorescence excitation at 563 nm of the conjugated dye to a standard dilution series (**Error! Reference source not found.** in the Supporting Information).

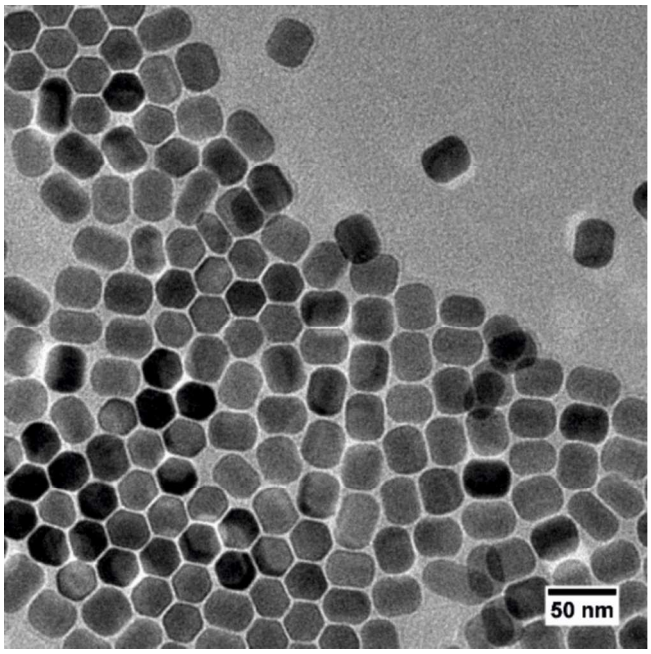

Figure 1. Transmission electron microscopy image of the upconverting nanoparticles with an average size of 28 ×36 nm (Tecnai 12 BioTwin TEM, 120 kV, FEI, Oregon, USA).

The pHrodo™ Red is a typical fluorogenic dye which fluorescence increases significantly due to protonation of the rhodamine chromophore, whereas other spectral properties (absorbance spectrum, emission wavelength) remain unaffected. The excitation energy of the UCNP at 550 nm is transferred to the pHrodo™ Red dye at least partly via an upconversion resonance energy transfer (UC-RET) process and its pH-dependent emission is then measured at 590 nm (Figure 2). Thus, a UCNP-sensitized emission of the pH indicator can be observed upon near infrared excitation at 980 nm.

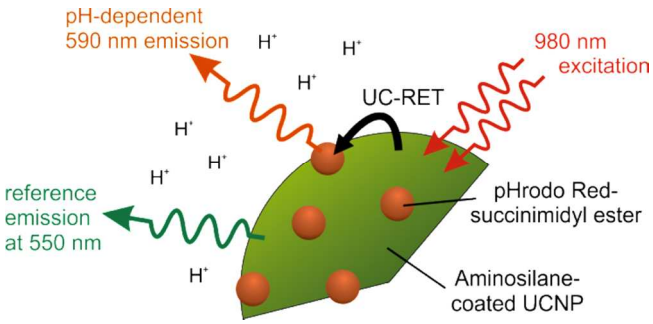

Figure 2. Schematic illustration of the photon upconversion based pH-sensor. The pH-sensitive pHrodo™ Red-succinimidyl ester is conjugated to the aminogroups of the silane-coated UCNP. The upconversion resonance energy transfer (UC-RET)-sensitized pH-dependent 590 nm emission of the pHrodo™ Red is measured upon 980-nm excitation. The pH-independent 550 nm emission of the UCNP is used as reference signal.

The upconversion photoluminescence spectrum was measured upon 980 nm excitation in pH 7.62 and 3.23 (Figure 3a). The photoluminescence intensity of the UCNPs was not affected by the pH which thus can be used as a reference signal for the calculation of the ratiometric response to pH. Also, the decrease of emission intensity at 550 nm due to UC-RET is not detectable due to the large number of emitting ions inside the nanoparticle. The sensitized

emission of the pHrodo™ Red -dye is hardly observable in the spectrum because the intensity of the upconversion photoluminescence exceeded the intensity of the indicator dye emission at least by factor of 50. Hence, for the measurement of the sensitized pHrodo™ Red emission the concentration of the UCNP-pHrodo™ Red -conjugate was increased ten-fold which caused the upconversion photoluminescence at both 550 and 660 nm to saturate the photo multiplier tube (Figure 3b). However, the pH-dependent emission of the sensitized dye became clearly distinguishable at these conditions.

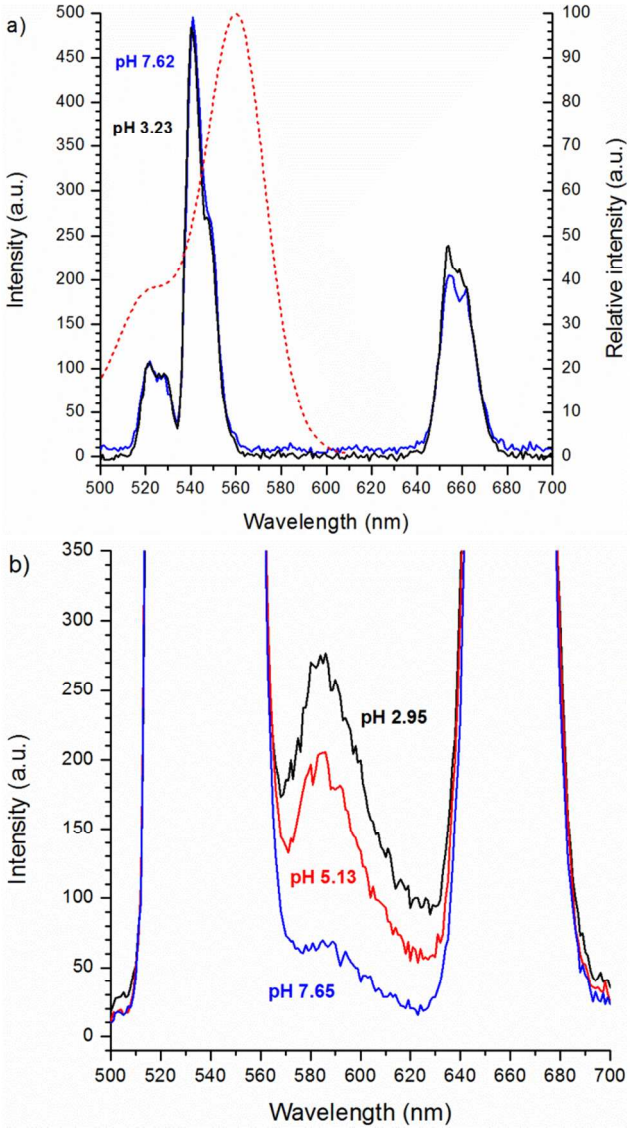

Figure 3. Emission spectrum of UCNP-pHrodo™ Red-conjugate upon 980 nm excitation. a) Emission spectrum of UCNP-pHrodo™ Red-conjugate in pH 7.62 and 3.23 (c = 0.1 mg/ml). The excitation spectrum of pHrodo Red (red dotted line, right y-axis) is overlaid with the emission spectrum of the UCNP. b) Sensitized emission spectrum of pHrodo™ Red in pH 7.65, 5.13 and 2.95 (c = 1 mg/ml).

The zeta potentials and the particle sizes of the UCNP-pHrodo™ conjugates were also measured at different pHs. The results are summarized in Table 1. **Error! Reference source not found.** shows the change of the size distribution by number at pH 7.0 and 3.8 over time after ultrasonication measured by dynamic light scattering (DLS). The conjugate is colloidally stable in pH 7 with the measured particle size of 37 ± 14 nm ten minutes after ultrasonication. No change of the size distribution could be observed after one hour. In decreasing pH, however, the particles tend to aggregate over time. Thus, in pH 3.75 the average particle size was measured to be 142 ± 99 nm after 10 minutes and 1514 ± 43 nm after 90 minutes.

Table 1. Size distribution by number (obtained by dynamic light scattering) and zeta potentials of the nanoprobe in different pHs.

pH	7.0	5.7	4.8	3.8
Size distribution (nm)*	37 ± 14	85 ± 44	120 ± 102	142 ± 99
Zeta potential (mW)	- 8.2	- 4.0	- 0.4	+ 9.7

*10 minutes after ultrasonication

The corresponding zeta potentials were -8.2 mV (pH 7.0) and +9.7 mV (pH 3.8), measured after ultrasonication. Even though the pHrodo™ Red dye is cationic, the measured zeta potential at pH 7.0 was negative. This was due to the higher abundance of acidic silanols than basic amines on the surface, which is a typical implication following co-condensation reactions. Nevertheless, the zeta potential of silica coated nanoparticles is still much more negative at pH 7, typically around -40 mV.[29] We also measured the zeta potential of the aminosilane coated UCNP before conjugation of the dye for comparison, which was -22 mV at pH 7.2 and +1.2 mV at pH 3.8. This indicates that the conjugated cationic dye has a significant impact on the surface properties of the nanoparticles, with a more pronounced positive surface charge contribution compared to the amino groups consumed in the conjugation. It should be noted that the presence of BSA in the storage buffer can have some impact on these results. The amount of amino groups could certainly be increased for a more efficient dye conjugation, albeit a too dense coverage of dye molecules can result in self-quenching.

The upconversion photoluminescence decays were measured from both amino-modified UCNPs and the UCNP-pHrodo™ Red-conjugate to confirm the UC-RET phenomenon. The emission was collected at 550 nm after a 2 ms excitation pulse of 980 nm. The data was analyzed by fitting the obtained signals of the UCNP-amino and the UCNP-pHrodo™ Red-conjugate simultaneously. As a result, two lifetimes were found to be the same (213 and 454 µs) which originate from the emitting ions that do not participate in the UC-RET-process. The third lifetime of the UCNP-amino was 94.0 µs and it decreased to 58.6 µs in the dye-conjugated sample. This decrease of 35.4 µs (Figure 4, insert) indicates that a nonradiative RET between the UCNP and pHrodo™

Red contributes to the sensitizing process. The UC-RET-efficiency η was 0.377 which was calculated according to the equation 1. This clearly distinguishes the sensing mechanism from previous approaches, where the absorbance of a pH indicator was used to attenuate the UCNP emission by reabsorption.[25]

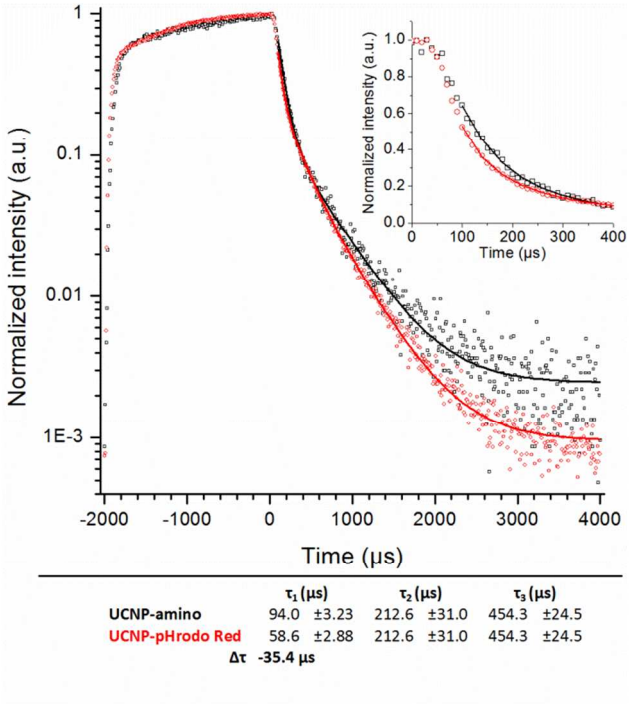

Figure 4. Upconversion photoluminescence decay curves of both UCNPs with amino-surface and UCNP-pHrodo™ Red-conjugate measured at 550 nm. The time range of 0–400 µs in linear range is shown in the insert.

$$\eta(\text{UC-RET}) = 1 - \frac{\tau(\text{UCNP-pHrodo}^{\text{™}}\ \text{Red})}{\tau(\text{UCNP})} \qquad (1)$$

pH-nanosensor

The presented pH-nanosensor can be used in a dynamic range between pH 7.2 and 2.5 with a linear ratiometric response between pH 3 and 6.7 when titrated with citrate (Figure 5). The sensor was referenced with the 550 nm emission of the UCNPs which is virtually not attenuated by UC-RET-process. (Figure 3a) This is due to the low amount of acceptor dyes and a large number of emitting ions in the nanoparticle that do not participate in the UC-RET. Note, that the 550 nm signal was attenuated by an OD 2 filter. If the amount of the acceptor dye on the UCNP surface was increased and the decrease in UCNP emission became significant, the sensor can alternatively be referenced also with the 660 nm emission which does not take part in the UC-RET.

The upconversion luminescence at 550 nm is not affected by the pH as such (**Error! Reference source not found.**a) and thus it could be used as a reference for ratiometric readout. However, at low pH aggregation of the particles can be observed over time, which leads to a slight increase of the emission (**Error! Reference source not found.**a). The increased emission, however, also increased the rate of energy transfer to the acceptor (**Error! Reference source not found.**b), keeping the ratiometric readout linear (**Error! Reference source not found.**c).

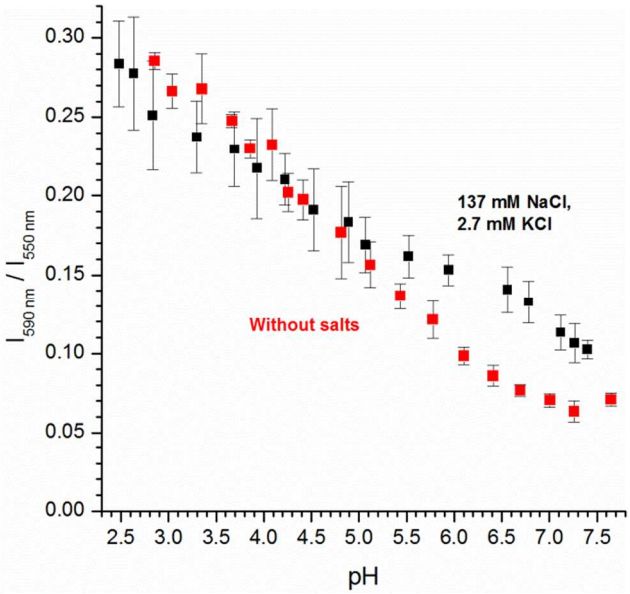

Figure 5. Ratiometric pH-titration curves of UCNP-pHrodo™ Red with and without a physiological salt concentration. pH was titrated by adding citrate and the ratio of the intensities of the sensitized emission of pHrodo™ Red at 590 nm and the 550 nm emission of the UCNP was calculated.

The standard deviations of the measured intensity ratios were high due to the titration method in which the pH was changed by adding citrate to three replicate wells. The added volume of citrate solution varied from 0.2 to 2 µl depending on the buffering capacity. The standard deviation of the measured pH at different steps varied from 0.02 to 0.19 units. The calibration of the pH response was also performed by diluting the UCNP-pHrodo™ Red conjugate to a series of buffers with different pHs. This decreased the standard deviations of the measured emission intensities of both the donor and the acceptor (**Error! Reference source not found.**a, b).From the linear range of the calibration the resolution (precision) of pH determination can be calculated to ± 0.3 (3 x SD / slope).

The pH-nanosensor was also tested with intracellular ion concentrations (137 mM NaCl and 2.7 mM KCl). Ionic strength is known to cause interferences with indicators for pH.[30] Also in this case the ionic strength affected the ratiometric response by decreasing the slope of the calibration plot and therefore the resolution of the sensor, but nevertheless the response was still nearly linear in the same pH range as without salts (Figure 5). The standard deviation of the intensities increased in saline, especially at low pHs.

The pH-sensor was also imaged with Leica SP5 STED confocal fluorescence microscope by scanning the emission at 550 nm and 590 nm upon 980-nm excitation from a droplet (V = 50 µL) with a particle concentration 0.02 mg/ml in buffered saline at different pH on a glass slide (**Error! Reference source not found.**). Single particles cannot be resolved under these conditions. Thus, at pH 7.1 only a few small aggregates can be found, whereas at pH 3.6 a high number of large aggregates appear. This is in agreement with the DLS experiments. Further, we used the aggregates to test the signal response and evaluate the scanning microscope for ratiometric measurements (Figure S4). The effect of increasing signal intensities due to aggregation at lower pH is compensated by the dual wavelength measurement. The photomultipliers of the 550 nm and 590 nm channels had different gain voltages to yield an almost equal ratio of both intensities at pH 3.6. No crosstalk of the UCNP emission to the red channel was observed.

A linear ratiometric pH-response can be obtained by analyzing single aggregates in the sample. The corresponding intensity ratios were quantified from the two emission channels of the microscopy images, resulting in a similar response as obtained in the microwell plate measurements.

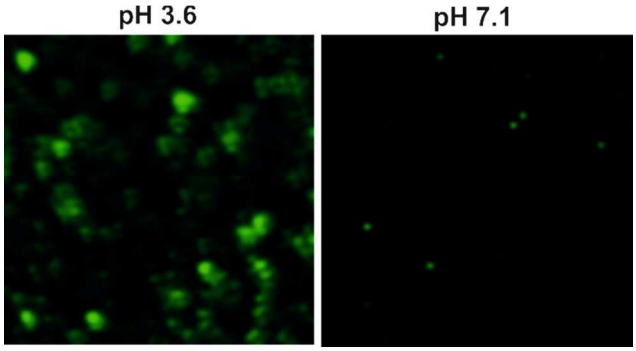

Figure 6. Fluorescence microscope images of the green emission of UCNP-pHrodo™ in droplets of 50 µL at different pHs on a glass substrate. The scanning area is 640 x 640 µm.

The cellular uptake of the particles into HeLa cells was examined by confocal microscopy (Figure 7). The UCNPs were efficiently taken up by the cells with a ratio of UCNP-positive cells of over 90% (Figure S5) and the green reference signal as well as the red pH-dependent signals could be detected. In the cells both individual particles and particle clusters were visible. Particle clustering is likely due to endosomal compartmentalization of the particles and cluster size increases as early endosomes fuse to larger late endosomes and possibly further to form multivesicular bodies. Both late endosomes and larger vesicular bodies would lead to the observed nanoparticle clusters.[31] Nevertheless, we observed also smaller, diffraction-limited signals that may originate from single nanoprobes. Over a period of 16 h no cytotoxic effects of the nanoprobes were observed with the highest particle concentration of 50 µg/ml (Figure S5). Loading of cells was typically performed with a particle concentration of 10 µg/ml. These experiments show that the pH nanoprobes are cell permeable and ratiometric signals can be obtained. A qualitative evaluation of the pH response inside cells can be found in the Supporting

Infromation (Figuere S 6), where the signals obtained from the culture medium outside the cells (pH 7.4) were used as reference. The increase of the pH-sensitive red emission of particles located in endosomes are clearly visible.

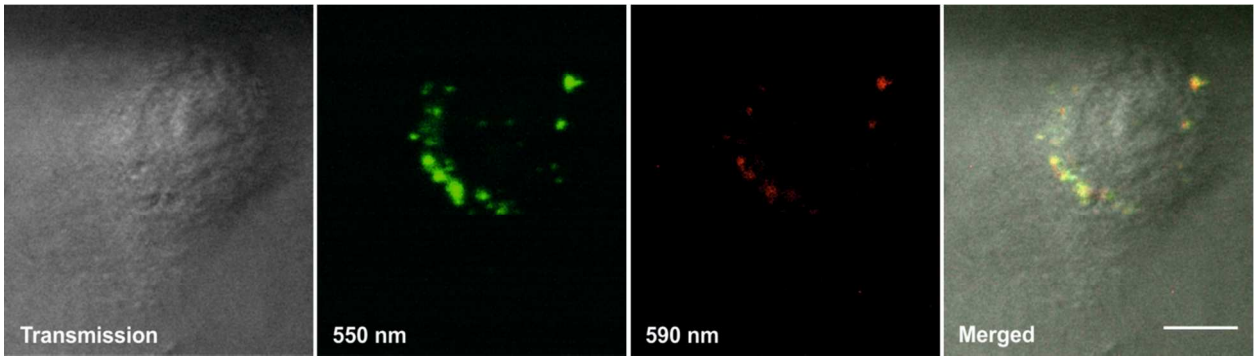

Figure 7. Transmission microscope image of a HeLa cell (left) and fluorescence images of the green emission (550 nm) and red emission (590 nm) of the nanoprobes internalized by the cell. The right image shows the transmission picture superimposed with the green and the red channel. A yellow color indicates a stronger red signal, and therefore, an acidic pH. The white scale bar is 10 µm.

3 Conclusion

In this work we introduced a simple, fast and sensitive pH-nanosensor based on upconversion photoluminescence resonance energy transfer between a nanosized UCNP-donor and a pH-sensitive pHrodo™ Red dye conjugated on the surface of the nanoparticle. The response is virtually linear in pH-range of 3–6.7 with a resolution of ± 0.3 pH. The dual wavelength pH nanosensor can be referenced by the donor UCNP emission which makes the results independent from the concentration and possible aggregation of the particles. The ratiometric measurement also eliminates interferences caused by variations of the excitation light intensity.

Due to the near-infrared excitation the presented system could be used as a pH-nanosensor to measure acidic pHs of intracellular compartments, e.g. of lysosomes. The silica coated UCNPs are biocompatible, easily functionalized, colloidal and extremely photostable. No photobleaching of the sensitized 590 nm emission could be observed after 90 minutes continuous illumination with a 980 nm laser (~95 mW). The nature of the upconversion photoluminescence also offers low autofluorescence background and deep light penetration into tissue. The applicability of the pH nanosensor as a probe for optical imaging was demonstrated by the scanning of HeLa cells loaded with particles with a confocal fluorescence microscope. Signals from both channels could be obtained. However, extensive calibration experiments and further optimization of the particles have to be performed to be able to use the ratiometric signal for a quantitative determination of pH inside cells. Therefore, we also intend to improve the sensitivity of the pH response by amplifying the sensitized red emission of the pH indicator. This can be achieved by the increase of the FRET efficiency due to the preparation of thinner silica shells or of the amount of conjugated indicators using highly amino-functionalized polymer coatings such as branched polyethyleneimine as binding matrix.

4 Experimental

Materials

Citric acid monohydrate, disodium phosphate ($Na_2HPO_4 \times 7\ H_2O$), tetramethyl orthosilicate (TMOS, ≥99 % purity), (N-(3-trimethoxysilyl)propyl)ethylene diamine (TMED, 97% purity), dimethyl sulfoxide (DMSO), 2-(N-morpholino)ethanesulfonic acid (MES), sodium bicarbonate ($NaHCO_3$), Trizma base and NaN_3 were purchased from Sigma-Aldrich (St. Louis, MO). Tween-85 was from Merck Millipore (Germany). Bovine serum albumin (BSA) was purchased from

Bioreba (Switzerland). A pH-sensitive dye pHrodo™ Red (M = 650 g/mol, ε = 65 000 $cm^{-1}M^{-1}$) was from Molecular Probes (Carlsbad, CA) and its structure has been published by *Ogawa et al*.[28] 30K Macrosep Advance centrifugal devices were from Pall Life Sciences (Omega, Ann Arbor, MI) and Thermo Scientific Nunc MaxiSorp microtiter wells from Thermo Fisher Scientific (Waltham, MA).

Synthesis of UCNP-pHrodo™ Red conjugate

The upconverting $NaYF_4$: Yb^{3+}, Er^{3+} (X_{Yb} 0.17, X_{Er} 0.03) nanophosphors, 28×36 nm in diameter (Figure 1), were synthesized in organic oils[26] and silanized with TMOS and TMED in 1:4 volume ratio to introduce primary amino groups as described previously[27] The size of the UCNPs was calculated from transmission electron microscopy (TEM) image by measuring the diameters of hundred particles with ImageJ software, version 1.43s (http://rsb.info.nih.gov/ij/).

The pH-sensitive dye pHrodo™ Red was conjugated covalently to the amino groups of the silica-coated UCNPs. Briefly, 3 mg of UCNPs in 474 µl of a 100 mM $NaHCO_3$-buffer (pH 8.5) was mixed with 200 nmol of pHrodo™ Red succinimidyl (NHS) ester in 26 µl of DMSO and incubated overnight protected from light in rotation in room temperature. The conjugate was washed twice with 500 µl of 10 mM Tris, pH 8.5, 0.1% Tween-20 by filtrating the conjugate solution with 30K Macrosep Advance centrifugal device and adding the buffer on top of the filter. The washed conjugate was finally suspended in 500 µl of 5 mM Tris, pH 8.5, 0.05% Tween-85, 0.5% BSA, 0.05% NaN_3 and stored at +4°C.

Characterization of the UCNP-pHrodo™ red -conjugate

The upconversion photoluminescence spectrum of the UCNP-pHrodo™ Red-conjugate was measured in different pHs (200 mM phosphate-citrate, pH 3.23, 5.34 and 7.62) with Cary Eclipse Fluorescence Spectrophotometer (Agilent Technologies, Santa Clara, CA) equipped with a 980 nm laser diode (~95 mW).[32] The emission spectrum was measured from 500 to 700 nm with 1 nm data interval, 5 nm emission slit and S/N mode. 0.1 mg/ml of UCNP-pHrodo™ Red-conjugate was used for the measurement of the UCNP-spectrum and 1 mg/ml UCNP-dye-conjugate was used for the visualization of the UC-RET-sensitized spectrum of the pHrodo™ Red dye.

The particle size, colloidal stability and zeta potential of the UCNP-pHrodo™ Red-conjugate were measured in 0.01 mg/ml concentration in 25 mM MES-buffer (pH 3.75, 5.72 and 7), 150 mM NaCl with Malvern Zetasizer Nano ZS (Malvern Instruments, UK). The zeta potential measurements were performed right after the sample was ultrasonicated for 5 min with a Covaris Acoustic Ultrasonicator (Covaris, Woburn, MA) and again after 10 minutes and >30 minutes to study the effect of pH on the colloidal stability. The particle size was measured by dynamic light scattering after ~5 min, ~10 min and ~90 min from the ultrasonication.

The time-domain lifetime of the upconversion photoluminescence of both the silanized UCNP-amino and the UCNP-pHrodo™ Red-conjugate was measured using the lifetime measurement mode of modified Plate Chameleon measurement device (Hidex Oy, Finland) equipped with a 980-nm laser diode.[31] The sample was repeatedly exposed to 2 ms excitation light pulses after which the decay of the upconversion photoluminescence at 550 nm was measured. The lifetime data was analyzed with Origin 8 (OriginLab, Northampton, MA) and exponential decay fitting.

pH nanosensor calibration

The UCNP-pHrodo™ Red-conjugate was diluted to a concentration of 0.015 mg/ml in 200 mM phosphate-citrate buffer with pH 7.65 in three replicas. The pH was titrated by adding 0.2 M citrate and the pH was measured with SevenEasy pH-meter (Mettler Toledo, Columbus, OH) equipped with InLab®423 Combination pH Micro Electrode (Mettler Toledo). Both the upconversion photoluminescence of the UCNP at 550 nm and the UC-RET-sensitized emission of the pHrodo™ Red at 590 nm were measured with clear MaxiSorp microwell plates using a modified Plate Chameleon reader (Hidex Oy). 100-fold attenuation was used for the 550 nm measurement by adding an optical density filter (OD 2, Thorlabs, Newton, NJ). The ratio of the luminescence intensity at 590 nm to 550 nm was calculated. The pH-titration was made in 200 mM phosphate-citrate buffer, pH 7.38 with a cellular salt concentration (137 mM NaCl, 2.7 KCl) and the different pH were adjusted by stepwise adding of 2 M citrate.

Fluorescence imaging

The UNCP-pHrodo™ Red-conjugate was imaged with Leica TCS SP5 STED Laser scanning microscope (Leica Microsystems GmbH, Germany) with Spectra-Physics Mai Tai Ti:Sapphire laser (Newport, Santa Clara, CA) adjusted to 980 nm for excitation at 25 % power. The UCNP-pHrodo™ Red-conjugate samples were dropped on a microscope slide with volumes of 50 µl in three different saline buffers of pH 7.1, 5.0 and 3.6. The emissions of the UCNPs and the pHrodo™ Red were scanned at 10 Hz rate with channels 525/50 nm (TRITC filter) with a confocal gain of 600 V of the PMT and 585/40 nm (FITC filter) with a confocal gain of 900 V of the PMT, respectively. The laser power was calculated to be 90 W mm^{-2}. The image analysis and quantification from both channels were performed with ImageJ software and the ratiometric signal was calculated.

Cellular imaging

HeLa cells were cultured in *Dulbecco's Modified Eagle's medium* (*DMEM*) (Life Technologies) with 10% fetal calf serum (FCS), 100 IU/ml penicillin, and 100 µg/ml streptomycin. UCNPs were added to cells in 2% FCS DMEM in concentration of 50 µg/ml and incubated for 16 h. The cells were cultured in glass bottom 96-well plates and the imaging was done on live cells, using also the Leica SP5 microscope. In this case, a 63X water objective (Leica) was used, with a GaAs-hybrid detector (Leica) for the red rhodamine FRET-signal and a standard PMT (Leica) for the green upconversion signal.

Before addition to the culture medium, the UCNPs (c = 4.5 mg/mL) were treated with branched polyethylenimine (c = 0.45 mg/mL) with an average M_W of 25000 (Sigma Aldrich) in 25 mM HEPES buffer containing 100 mN NaCl. The mixture was rotated overnight and the particles were collected by centrifugation (30 min, 14000 rpm) and washed twice with HEPES.

Supporting Information. The determination of the amount of pHrodo™ Red conjugated to the particles, and the results from pH calibration showing the response at 550 nm, 590 nm and ratiometric, is available in the Supporting Information. These also contain the results of the DLS measurements showing the aggregation of particles over time at acidic pH, the ratiometric imaging test with the scanning microscope, and the cellular uptake.

Acknowledgement

This study was supported by Tekes, the Finnish Funding Agency for Technology and Innovation. The authors would like to acknowledge Emilia Palo for synthesizing the UCNPs and Satu Lahtinen for silanizing the UCNP. This work made use of the Aalto University nanomicroscopy Center (Aalto-NMC) premises.

Abbreviations

BODIPY, boron-dipyrromethene; HPTS, 8-hydroxypyrene-1,3,6-trisulfonic acid; NIR, near-infrared; UCNP, upconverting nanoparticle, UC-RET, upconversion resonance energy transfer; DLS, dynamic light scattering; TMOS, tetramethyl orthosilicate; TMED, (N-(3-trimethxysilyl)propyl)ethylene diamine; DMSO, dimethyl sulfoxide; MES, 2-(N-morpholino)ethanesulfonic acid; BSA, bovine serum albumin; TEM, transmission electron microscopy

References

1 J. Han, K. Burgess, *Chem. Rev.* **2010**, *110*, 2709–2728.

2 A. Burns, B. Sengupta, T. Zedayko, B. Baird, U. Wiesner, *Small,* **2006**, *2*, 723–726.

3 L. Shang, G.U. Nienhaus, *Materials Today*, **2013**, *16*, 58–66.

4 Y.-E. Koo Lee, R. Kopelman, *Wiley Interdiscipl. Rev. Nanomed. Nanobiotechnol.* **2009**, *1* 98–110.

5 Y.-E. Lee Koo, Y. Cao, R. Kopelman, S.M. Koo, M. Brasuel, M.A. Philbert, *Anal. Chem.* **2004**, *76*, 2498–2505.

6 J. Napp, T. Behnke, L.H. Fischer, C. Würth, M. Wottawa, D.M. Katschinski, F. Alves, U. Resch-Genger, M. Schäferling, *Anal. Chem.* **2011**, *83*, 9039–9046.

7 H.A. Clark, M. Hoyer, M.A. Philbert, R. Kopelman, *Anal. Chem*. **1999**, *71*, 4831–4836.

8 S. Hornig, C. Biskup, A. Gräfe, J. Wotschadlo, T. Liebert, G.J. Mohr, T. Heinze, *Soft Matter* **2008**, *4*, 1169–1172.

9 M. Bradley, L. Alexander, K. Duncan, M. Chennaoui, A.C. Jones, R.M. Sánchez-Martín, *Bioorg. Med. Chem. Lett.* **2008**, *18*, 313–317.

10 Y.-S.Liu, Y. Sun, P.T. Vernier, C.-H. Liang, S.Y.C. Chong, M.A. Gundersen, *J. Phys. Chem. C* **2007**, *111*, 2872–2878.

11 X.d. Wang, J.A. Stolwijk, T. Lang, M. Sperber, R.J. Meier, J. Wegener, O.S. Wolfbeis, *J. Am. Chem. Soc.* **2012**, *134*, 17011–17014.

12 K. Kuningas, H. Päkkilä, T. Ukonaho, T. Rantanen, T. Lövgren, T. Soukka, *Clin. Chem.* **2008**, *53*, 145–146.

13 M. Nyk, R. Kumar, T.Y. Ohulchanskyy, E.J. Bergey, P.N. Prasad, *Nano Lett.* **2008**, 8334–3838.

14 T. Rantanen, M.-L. Järvenpää, J. Vuojola, R. Arppe, K. Kuningas, T. Soukka, *Analyst* **2009,** *134*, 1713–1716.

15 T. Rantanen, M.-L. Järvenpää, J. Vuojola, K. Kuningas, T. Soukka, *Angew. Chem. Int. Ed.* **2008**, *47*, 3811–3813.

16 Y. Wang, K. Liu, X. Liu, K. Dohnalová, T. Gregorkiewicz, X. Kong, M.c.g. Aalders, W.J. Buma, H. Zhang, *J. Phys. Chem. Lett.* **2011**, *2*, 2083–2088.

17 J. Chen, H. Chen, C. Zhou, J. Xu, F. Yuan, L. Wang, *Anal. Chim. Acta* **2012**, *713*, 111–114.

18 S. Jiang, Y. Zhang, *Langmuir* **2010**, *26*, 6689–6694.

19 F. Zhou, M.O. Noor, U.J. Krull, *Anal. Chem.* **2014**, *86*, 2719–2726.

20 H. Li, L. Wang, *Analyst* **2013**, *138*, 1589–1595.

21 J. Zhang, B. Li, L. Zhang, H. Jiang, *Chem. Comm.* **2012**, *48*, 4860–4862.

22 S. Hao, G. Chen, C. Yang, *Theranostics*, **2013**, *3*, 331–345.

23 H.S. Mader, O.S. Wolfbeis, *Anal. Chem.* **2010**, *82*, 5002–5004.

24 R. Ali, S.M. Saleh, R.J. Meier, H.A. Azab, I.I. Abdelgawad, O.S. Wolfbeis, *Sensors Actuat. B.* **2010**, *150*, 126–131.

25 T.V. Esipova, X. Ye, J.E. Collins, S. Sakadzic, E.T. Mandeville, C.B. Murray, S.A. Vinogradov, *Proc. Nat. Acad. Sci. USA* **2012**, *109*, 20826–20831.

26 M. Ylihärsilä, E. Harju, R. Arppe, L. Hattara, J. Hölsä, P. Saviranta, T. Soukka, M. Waris, *Clin. Microbiol. Infect.* **2012**, *19*, 551.

27 R. Arppe, O. Salovaara, L. Mattsson, S. Lahtinen, T. Valta, T.Riuttamäki, T. Soukka, *J. Nanopart. Res.* **2013**, *15*, 1883.

28 M. Ogawa, N. Kosaka, C.A.S. Regino, M. Mitsunaga, P.L. Choyke, H. Kobayashi, *Mol. Biosyst.* **2010**, *6*, 888–893.

29 E. Mahon, D.R. Hristov, K.A. Dawson; *Chem. Commun.* **2012**, *48*, 7970–7972.

30 B.M. Weidgans, C. Krause, I. Klimant, O.S. Wolfbeis, *Analyst*, **2004**, *129*, 645–650.

31 N. Prabhakar, T. Näreoja, E., von Haartman D.S. Karaman, H. Jiang, S, Koho, T.A. Dolenko, P.E. Hänninen, D.I. Vlasov V.G. Ralchenko, S.Hosomi,. I. Vlasov, C. Sahlgren, J.M. Rosenholm, *Nanoscale* **2013** *9*, 3713-3722

32 T. Soukka, K. Kuningas, T. Rantanen, V. Haaslahti, T. Lövgren, **2005**, *15*, 513–528.